doi:10.2533/chimia.2024.333 Chimia 78 (2024) 333–338

Operando Neutron Imaging

Marin Nikolic, Alessia Cesarini, Ali J. Saadun, Eric R. Carrein Ruiz, Andreas Borgschulte*, Pavel Trtik, and Pierre Boillat

Abstract: In the past, neutron imaging has been the little brother of advanced neutron spectroscopy techniques due to its apparent simplicity. However, this simplicity allows the studying of complex chemical and electrochemical processes and related devices even under harsh reaction conditions such as high pressure, high temperature, corrosive and/or air sensitive environments. We review a number of highly relevant case studies as archetypal examples of modern energy technology; that is heat storage, power-to-X, batteries, fuel cells, and catalysis. The promising results trigger the further development of neutron imaging towards a chemical imaging method.

Keywords: Catalysis · Electrochemistry · Fuel cells · Neutron imaging · Power-to-X

Pierre Boillat, Andreas Borgschulte, and Pavel Trtik working on the manuscript.

Pierre Boillat has been working on neutron imaging of electrochemical devices since 2005 and received a doctorate from the ETH Zurich in 2009. He holds a joint appointment at the Paul Scherrer Institut (PSI) between the Electrochemistry Laboratory and the Laboratory for Neutron Scattering and Imaging. His work encompasses both the advancement of the neutron imaging methodology, including the development of spectroscopic imaging, and the application of the developed techniques to understand the limitations of electrochemical devices.

Andreas Borgschulte is a physicist with a focus on Applied Spectroscopy. He received his doctorate in physics from TU Braunschweig, Germany in 2002. After postdoctoral position at VU Amsterdam and the Helmholtzzentrum Geesthacht, Germany, he started exploring the hydrogen world as a group leader of the group Hydrogen Spectroscopy at Empa. He shares his ideas and experience as lecturer at University Zurich and ETH Zurich.

Pavel Trtik is a beamline scientist at the thermal neutron imaging instrument NEUTRA at the Paul Scherrer Institute (PSI), Switzerland. He was also responsible for the development of the high resolution neutron detector (called 'PSI Neutron Microscope') that significantly pushed the boundaries of the achievable spatial resolution of neutron imaging. He received his PhD from the University of Paisley, Scotland in the field of materials science of cement-based materials and since being at PSI his research interest naturally broadened to a wide scope of topics addressable by (high-resolution) neutron imaging.

*Correspondence: Dr. A. Borgschulte, E-mail: andreas.borgschulte@empa.ch
Empa Dübendorf, CH-8600 Dübendorf

Eric Ricardo Carreon Ruiz received his PhD in Chemistry from ETH Zurich in 2023. His research focuses on developing a novel characterization technique to study Li-ion battery materials *in situ*. This technique aims to understand the impact of extreme conditions on battery performance. His primary interest lies in alternative energy solutions and sustainable development.

Marin Nikolic received his Masters degree in Chemistry from the University of Zurich in 2018. His Master Thesis focused on the photo-electrochemical water splitting, which he did in the group of Prof. David Tilley. After the Masters, he gained two years of industrial work experience in Dow AG and in Dottikon ES AG. He started his PhD in late 2020 at Empa.

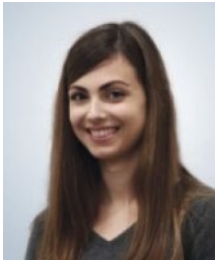

Alessia Cesarini studied at ETH Zurich, where she obtained her BSc and MSc degrees in chemistry. During her master studies she approached the field of catalysis with a thesis work on CO_2 conversion to CH_3OH. Afterwards, she began her doctoral studies in heterogeneous catalysis at Empa in collaboration with the Department of Chemical and Bioengineering, ETH Zurich (Prof. Dr. J. A. van Bokhoven). Her research focuses on developing new process for the conversion of light olefins in jet fuel range products.

Ali Saadun is a chemical engineer holding additionally an LLM in business law and an MSc in management. He obtained his PhD in chemical engineering from ETH Zurich in 2021. With a primary research interest in energy-related solutions, he embarked on his first postdoctoral position at Empa where he focused on advancing automotive lithium-ion batteries. He then transitioned to a second postdoctoral role at the same institute, shifting his emphasis to developing processes for sustainable transportation fuels.

1. Introduction

The world is in need for sustainable, economically and energetically efficient energy devices.[1] The performance of such devices hinges on the properties of the materials used on one hand, and on the details of the design on the other.[2] Although not uncommon, the independent development of new materials faces limitations, if they do not match boundary conditions given by the setup and concrete construction of the device.[3] In particular for energy devices, those boundary conditions are often visible under operational conditions only, and *operando* characterization is needed to understand the materials - device structure - performance relationship.[4]

Furthermore, real energy conversion and storage devices often need to be scaled-up to the multi-megawatt or even gigawatt range. To minimize effort, technology development proceeds over various development stages ('readiness levels') starting at small prototypes, before building the final large-size plant.[5] Tutorial example is the development of chemical reactors for, *e.g.* CO_2 methanation.[6] Catalyst development takes place in small research lab reactors. These reactors are designed to generate the conditions present in a large-scale reactor, that is, gas composition, pressure and temperature, which are supposed to be constant over the whole catalyst bed.[4] This is a working hypothesis introduced to simplify analysis, which does not stand up to closer scrutiny. Already at microscopic scale, concentration, potential and temperature gradients may exist, which reproduce with the growth in size.[7] The investigation of such effects require a chemically selective imaging method. Often, these effects are to be expected on a macroscopic scale, where the mass and/or heat transport becomes the rate-limiting factor.[7] A chemically selective method will help to understand both the local response of the active material as well as the overall performance of the energy device.[8,9] Two modes of operation are possible: structural studies of energy devices under operating conditions and true *operando* neutron imaging. In the first case, the performance of the device is obtained in a separate experiment and a similar behaviour is assumed during neutron imaging. As this approach has some uncertainties, the *operando* experiment is preferred, where the performance parameter is measured simultaneously with the structural investigation. Obviously, the effort for such a beamline experiment is much higher and not always possible. In this short review we give examples of both *modi operandi* for applications in heat storage, electrolysis, fuel cells, batteries and power-to-gas.

2. Fundamentals of Neutron Imaging

Neutron imaging makes use of the specific absorption and scattering cross section of neutrons for different materials.[10] Since neutrons are difficult to deflect, common configurations do not use focusing optics and are limited to a collimated neutron beam shining on the object of interest as close as possible to the imaging detector (Fig. 1).[11] The large neutron scattering cross section for hydrogen compared to other elements makes neutron radiography ideal as a non-destructive tool to probe gaseous as well as condensed hydrogen containing phases in the energy devices, often without the need to modify the setup to accommodate the imaging analysis.[12] Pressure limitations are severe constraints for many other *operando* methods based on photons and electrons, but do not impact neutron imaging, as the neutron beam penetrates easily thick reactor walls made of many metals (*e.g.* aluminum, titanium or even steel), making it the ideal method for *operando* chemical reactor analysis.[12]

Neutrons interact with the nucleii, and thus the scattering cross section is mainly element specific (σ_0) with a particularly high value for hydrogen. However, the total cross-section σ_H depends on the chemical environment of the proton (vibrational structure) as given by the scattering law.[13] As the vibrational structure is specific to the chemical structure, a heterogeneous distribution of different chemical compounds with the same number of elements leads to a measurable neutron imaging contrast. Most neutron imaging beam lines use polychromatic beams,[10] which reduces the overall chemical sensitivity. Nevertheless, there is a chemical contrast for hydrogen containing molecules with different binding.[14,15] Ultimately, monochromatic sources and/or energetically resolved neutron detection using, *e.g.* time-of-flight neutron imaging are ideal as a spatially resolved spectroscopic method for *operando* studies.[15]

Usually, the imaging method is used as radiography, *i.e.* the 3D-object is imaged by the 2D-neutron attenuation contrast image. The method can be extended to tomography.[16] A 3D neutron tomography image of the object is created by taking individual images from a number of different angles around its center axis. The data is then reconstructed to provide a 3D map of linear attenuation coefficients for each voxel.[16]

The spatial resolution of neutron imaging ranges from a few µm[17,18] to a few hundreds of µm. The resolution is usually related to the extension of the field of view, which can range from a few mm to tens of cm for the largest beams available. For objects with high aspect ratios, specific anisotropic setups have been used to allow high resolution in one direction while keeping a large field of view in the perpendicular direction.[19] The temporal resolution largely depends on the contrast, acceptable level of noise and required spatial resolution and is usually in the range of seconds, though it can go as low as a few ms in specific applications.[20]

A great advantage of neutron imaging is the negligible influence of temperature on the measurement, in contrast to, *e.g.* inelastic neutron scattering.[10] Thus, it is suited as an *operando* method, if combined with an analysis method determining the corresponding performance parameter simultaneously. This is typically a gas analyzer (infrared gas analysis or mass spectrometry) for gas reactions, or simply a potentiostat in case of electrochemical reactors (fuel cells, electrolyzers, batteries).

3. Neutron Imaging for Device Characterization

Several authors remember having difficulties in operating an Italian mocca machine for the first time. In contrast to ordinary filter machines, one cannot see the water flux, and thus the functioning principle is not obvious. *In situ* neutron imaging makes the water flux visible,[21] and now the authors can prepare proper

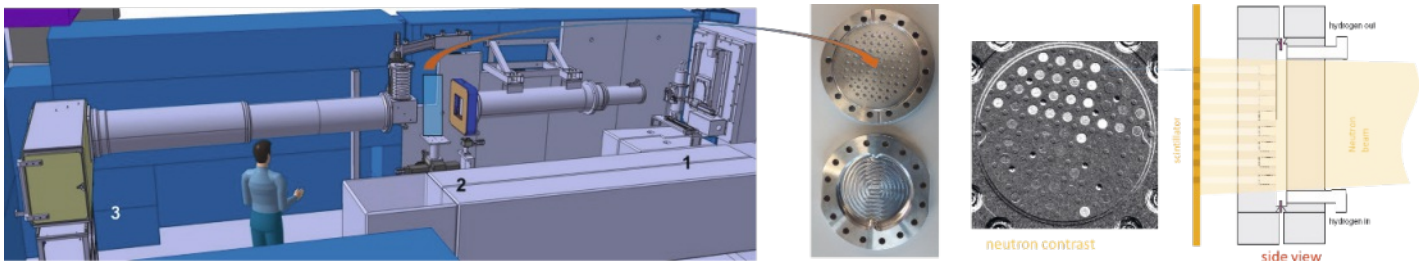

Fig. 1. Generic setup of a neutron imaging experiment. The object (reactor, battery, or combinatorial catalyst test reactor as shown here[36]) is placed in the neutron beam directly in front of a scintillator screen, which is read out by a camera.

coffee with an Italian mocca machine. In the following, we showcase similar technical examples, in which already the qualitative interpretation of the imaging results of the process gives valuable insights.

3.1 *Characterizing Liquid Mass Transport in Engineering Applications by Neutron Imaging Under Operation Conditions*

Mass transport in liquids is of the utmost technical importance. As the corresponding scientific fundamentals were established a long time ago (Navier-Stokes equations, diffusion equations), fundamental research is apparently not needed anymore, and most work focusses on their technical implementation, *e.g.* by computer modelling.[22]

However, full description and thus successful anticipation of new technical inventions is impeded by the incomplete knowledge of the various details of technical real-world systems. An example is heat storage in aqueous sodium hydroxide solutions, which is based on the heat of water absorption in the NaOH solution.[23] While the energy density is given by the heat of absorption and amount of reversibly exchanged water, the power performance depends on the interdependent heat and mass transport in the liquid, which is a complex function of the design of the device to optimize the varying density, viscosity, diffusion, heat conductivity, surface tension, of the solution.[24] As water vapor pressure and heat of absorption depend on water concentration and temperature, also the energy density of the heat storage is eventually limited by the power performance.[24]

Model experiments based on simplified geometries can be used to determine a basic relationship, *e.g.* of the rate-limiting step. Similarly, the corresponding materials properties are derived from special measurement apparatus. Apparently, all information to design an optimized heat storage device is available. In practice, though, the design is based on experience with heat and mass exchangers and/or trial and error, which may or may not lead to improved performance. Here, the *in situ* visualization of the mass flows in the solution is of tremendous help.[25]

Fig. 2 is a didactic example of how neutron imaging can determine the length scale of mass transport mechanisms in NaOD solutions. In addition to this straightforward geometry, the authors studied various other design setups. Best mass transport performance was achieved in optimized fin absorber structures.[25] Based on these observations, the authors constructed and tested a novel mass and heat exchanger with markedly improved area specific power and thermal energy storage density.[25]

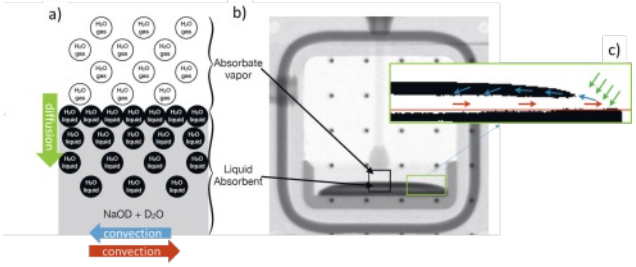

Fig. 2. a) Illustration of the principle to visualize mass transport in aqueous solution by neutron imaging. Light water (H_2O) with its higher neutron cross section is absorbed from the gas phase and diffuses into the deuterated NaOD solution droplet with lower neutron cross section. b) Neutron image of the cell showing the chamber vapor volume (H_2O gas), droplet supply and absorbent film (NaOD + D_2O). c) Snapshot of a neutron image during absorption demonstrating that diffusion is rate-limiting on small length scale, while convection is dominating on macroscopic scale. From ref. [25]

The concept study of water absorption in aqueous sodium hydroxide may serve as a blueprint for similar technical systems. Its applicability is defined by the contrast in neutron cross sections of the tracer to background (*e.g.* hydrogen to deuterium), total neutron attenuation, and the spatial resolution of the neutron imaging setup. While the latter 'hard' limits the minimum resolution to micrometers, the other parameters, which particularly limit the macroscopic dimension, have to be discussed on a case-by-case basis.

3.2 *Characterizing Mass Transport in Chemical Reactors by Operando Neutron Imaging*

The upscaling of chemical reactors is a time-and capital consuming challenge.[5] In most cases, the process is optimized on the lab scale. However, various processes such as heat and mass-transport are negligible or play a minor role only. These effects, which become dominating in large scale reactors, are usually considered by modelling (see Fig. 3). However, the number of technical parameters, which are unknown and/or have to optimized is huge. This is particularly relevant for novel processes, where practical experience is lacking. The sorption enhanced methanation

$$CO_{2,\,gas} + 4H_{2,\,gas} \rightarrow CH_{4,\,gas} + 2H_2O_{\,ads}$$

is an archetypal example. Here, the *in situ* removal of the product water improves reaction yield.[26] The principle has been known for a long time,[27] although there are only few large scale realizations. In contrast to the wide-spread plug-flow reactors, the number of products in the reactor (specifically water) defines the reactor performance. When we started R and D on this topic roughly 10 years ago,[26] we anticipated the water distribution in the reactor by comparison with similar reactions. It was expected that the water distribution follows a step function, with the step ('reaction front') moving with time. This qualitative behavior was indeed found by *operando* neutron imaging (Fig. 3).[28] Once the reaction front arrives at the exit of the reactor, the gas analysis detects unreacted CO_2, and the previously practically 100% conversion drops to the values achieved in an ordinary plug-flow reactor. In addition to the qualitative statement, the evaluation allowed us to quantitatively link the reaction yield with water distribution. The reaction front velocity is constant, although there is a final unequal water distribution. This indicates that the main effect of sorption enhancement is improving reaction kinetics only at low water partial pressures, later confirmed by lab experiments. The results were directly used to design an improved reactor prototype (Fig. 3).[30]

3.3 *Characterizing Batteries by Operando Neutron Imaging*

A battery is the technical realization of an electro-chemical reaction to store electricity. No doubt, the electrochemical phenomena are pivotal to develop a battery; however, the engineering of the final device adds an extra challenge. Electrode structuring and sizing, packaging, and housing need to be optimized while taking into account the changing state of charge (SoC) of the battery.[31] Obviously, *operando* methods are beneficial here. Fig. 4 shows a neutron radiography image of an Ni-metal hydride battery. In such batteries, electricity is stored by transferring hydrogen from a Ni hydroxide electrode to a rare-earth nickel electrode forming rare-earth nickel hydride and leaving Ni oxy-hydroxide behind.[32] During charging, the hydrogen concentration in the hydride electrode (full red dots) follows the accumulated charge in the battery (black line) up to a specific voltage (blue line). Here, hydrogen gas is formed, which is also detected by neutrons (hollow red points, Fig. 4[9]).

In addition to these global phenomena, neutron imaging is used to visualize local changes of the materials, be it the electrodes or the electrolyte. Here, new developments in neutron

imaging instrumentation opens new possibilities. In Fig. 5, the generally high selectivity of neutrons for hydrogen is utilized.

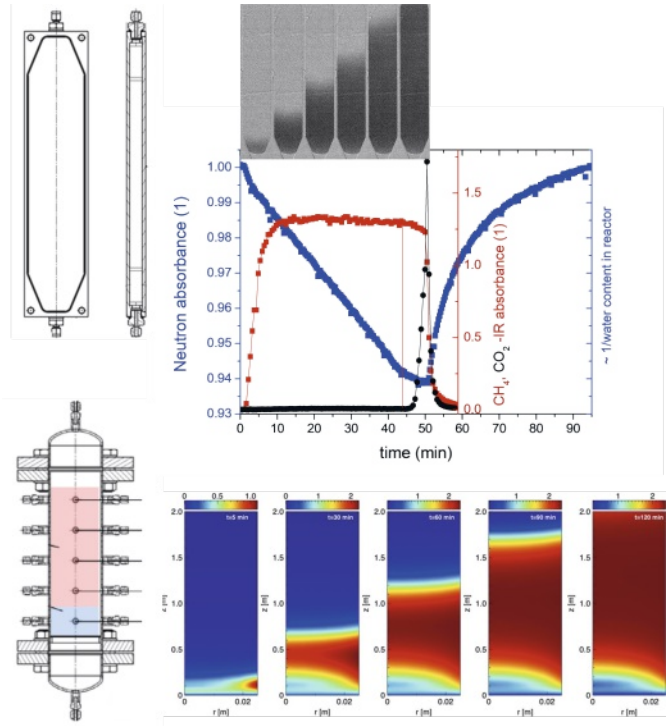

Fig. 3 a): Neutron contrast imaging during sorption enhanced methanation in 40 cm long planar model reactor. Distribution (black & white images) as well as total water content in a reactor is measured simultaneously with the reaction yield (CO_2 conversion and CH_4 yield). From ref. [28]. b) Simulations of the water content in a cylindrical reactor displayed as colour maps. From ref. [29].

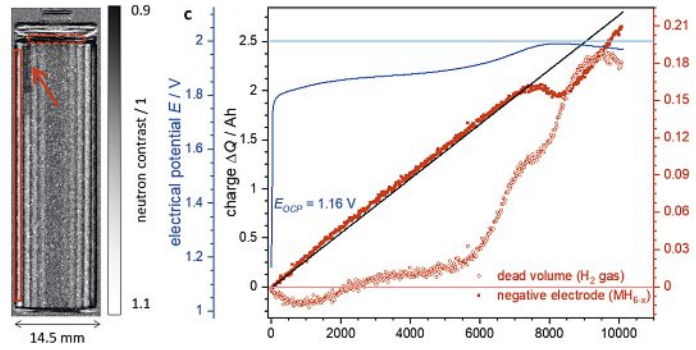

Fig. 4. Neutron absorption of the outer negative electrode (indicated by the red rectangle with a solid line in the neutron radiography of the battery and of the hydrogen gas in the top head space (indicated by the red rectangle with a dotted line in the neutron radiography of the battery as a function of time, *i.e.* at different SoC. The black is the accumulated charge. From ref. [9]

To increase the chemical contrast, time-of-flight neutron imaging exploits the wavelength-dependent properties of hydrogen atoms (Fig. 5, see also section 2). With this method, real-time physical and chemical changes in H-containing compounds can be followed *in situ*, supporting the development of new electrolyte mixtures and additives.[15,34]

3.4 *Characterizing Gas, Liquid and Ion Transport Fuel Cells and Electrolyzers by Operando Neutron Imaging*

Similar to batteries, fuel cells and electrolyzers are devices based on electrochemical conversion reactions. However, unlike

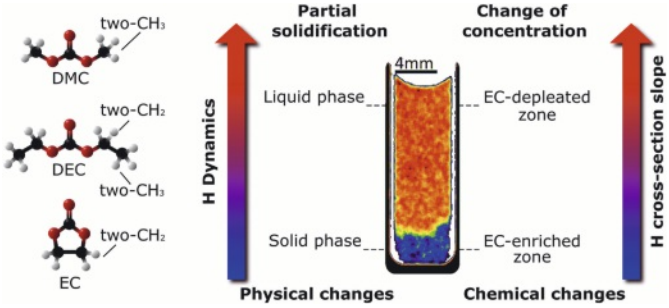

Fig. 5. Left: typical organic compounds used in battery electrolytes. In a battery, they can solidify, as well as segregate, both leading to a visible neutron contrast. From ref. [15]

batteries, they are open systems with reactants and products (*e.g.* hydrogen and water) stored and disposed outside of the device. In polymer electrolyte fuel cells, the formation of water is of utmost importance as a finite water concentration is needed for the polymer electrolyte membrane.[33] On the other hand, liquid water can block the access to active sites on the electrodes or disturb the distribution of gas flows and needs to be properly managed.

R and D follows various pathways: chemical surface modifications *e.g.* adding hydrophobic surfaces (teflon) to the porous media; and different design of the components such as the electrodes, gas diffusion layers, and bipolar plates. *In situ* characterization by neutron imaging helps visualizing the water distribution during operation and understand the effect of these design choices, as well as of the operating strategies, on liquid water management. Unfortunately, while the imaging of large channels in the gas-diffusion layer and bipolar plates does not pose a great difficulty, the imaging of the water distribution at the electrodes near to the membranes is limited by the finite spatial resolution of neutron imaging. Fig. 6 shows high-resolution *in situ* neutron imaging of a model PEM-fuel cell.[33] The high resolution of approximately 20 µm while keeping a sizeable field of view of 100 mm was achieved by an anisotropic imaging setup. As the measurements were made together with electrochemical control, a correlation between the water content and operating parameters such as the stability of operation and the pressure drop across the cell could be established.[19]

Recently, novel electrolyzers have been developed targeting the splitting of CO_2 and water. The number of intermediates and products including gaseous, liquid and even solid phases requires a careful chemical as well as structural characterization. *Operando* neutron imaging could provide new impetus here.[35]

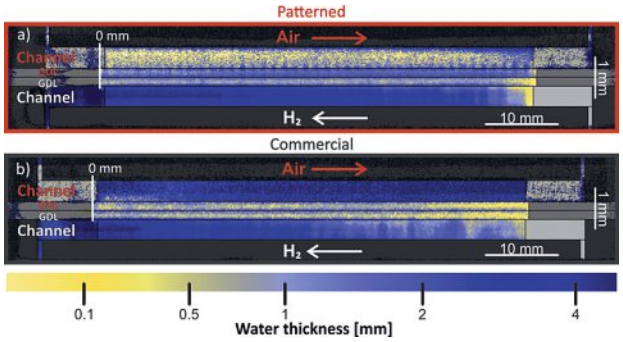

Fig. 6. Anisotropic radiography of the water content in the flow channels and porous media of operating fuel cells. A specially designed 'patterned' porous material is shown to significantly improve the water drainage from flow channels. From ref. [19].

3.5 *Combinatorial Research with Neutron Imaging*

Imaging procedures have been developed to spatially resolve materials' structures. However, neutron imaging is typically limited to a spatial resolution in the micrometer range.[18] If changes occur on length scales below this value, information can still be drawn from the measurements. As a tutorial example, Fig. 7 shows neutron contrast images of hydrogen exchanged by deuterium in a $Cu/ZnO/Al_2O_3$ catalyst pellet. The contrast (degree of H/D exchange) is time dependent, although no local differences are observed. This means that the rate-limiting step takes place on a length scale below the spatial limit of the neutron setup (50 μm). However, the absolute amount and its time dependence is relevant information, in particular, as it can be compared to the simultaneously measured reaction yield.[36]

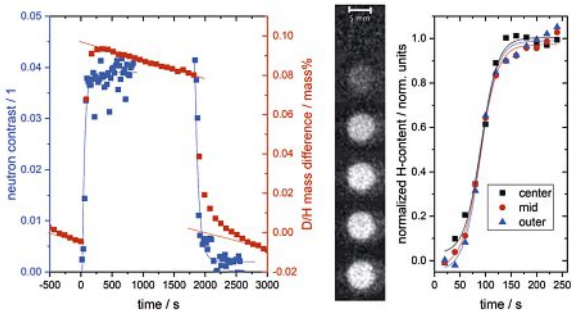

Fig. 7. Left graph: Averaged change of neutron contrast (blue squares) and mass (red squares) of a Cu/ZnO catalyst upon gas switch from hydrogen to deuterium and *vice versa* at 200 °C indicative of H/D exchange in the pellet. Right graph: Time- and spatially-resolved neutron contrast upon hydrogen deuterium exchange (at t = 0) derived from the neutron radiography image series (t = 0, 25, 50, 75, 100, and 250 s) at three different locations in the pellet (in the centre, at half radius and at maximum radius). From ref. [36].

To further interpret this result, such measurements need to be repeated at various conditions (gas composition/pressure/temperature) and for various catalysts. At best, this is performed for a great number of parameters, *i.e.* a high-throughput approach followed by combinatorial analysis. Imaging methods are ideal for this, as a great number of samples in a sample holder under identical conditions can be followed. The corresponding high-throughput aluminum reactor setup able to accommodate up to 69 samples is shown in Fig. 1.[36] Simplest reactions with highest neutron contrast is the already mentioned hydrogen deuterium exchange reaction, providing insights into the number of hydrogen on the catalyst surface, and whether it is present as absorbed hydrogen, mobile hydrogen or as pre-existing OH groups.[37] This method coined CONI (combinatorial neutron imaging) may be extended to other reactions, where the amount of hydrogen is relevant.

4. Conclusions

The few examples highlighted here illustrate the wide range of applications of neutron imaging for studying the possibilities and limitations of energy conversion and storage devices. We started with the apparently simple system of water absorption in aqueous NaOH solution, which is a showcase for neutron imaging under operation conditions. The usefulness of *operando* neutron imaging for chemical engineering is demonstrated along sorption enhanced methanation reactors. In both cases, the observation of pattern formation as a direct result from imaging helped in improving the corresponding device. Additional examples discussed are electrochemical devices, *i.e.* batteries, fuel cells and electrolyzers as showcases for chemically selective imaging with quantitative information. The latter can be used for combinatorial research with neutrons, where the imaging allows the simultaneous measurement of a multitude of samples (high-throughput approach). All examples demonstrate the applicability of neutron imaging either *operando* and/or under demanding reaction conditions.

Acknowledgements

Funding: Financial support from the Swiss National Science Foundation [Grant nos. 172662 and 182987] was greatly acknowledged. Additional funding from the UZH-UFSP program LightChEC and the ETHBoard *via* the mega-move and joined Empa-PSI Synfuel project was received.

Received: February 14, 2024

[1] a) R. E. Smalley, *MRS Bulletin* **2005**, *30*, 412, https://doi.org/10.1557/mrs2005.124.; b) IPCC, **2022**: Eds. P. R. Shukla, J. Skea, R. Slade, A. Al Khourdajie, R. van Diemen, D. McCollum, M. Pathak, S. Some, P. Vyas, R. Fradera, M. Belkacemi, A. Hasija, G. Lisboa, S. Luz, J. Malley 'Climate Change 2022: Mitigation of Climate Change. Contribution of Working Group III to the Sixth Assessment Report of the Intergovernmental Panel on Climate Change', Cambridge University Press, Cambridge, UK and New York, NY, USA;

[2] F. Blaabjerg, D. M. Ionel, *Electr. Power Comp. Syst.* **2015**, *43*, 1319, https://doi.org/10.1080/15325008.2015.1062819.

[3] A. Borgschulte, J. Terreni, B. Fumey, O. Sambalova, E. Billeter, *Front. Energy Res.* **2022**, *9*, 784082, https://doi.org/10.3389/fenrg.2021.784082.

[4] S. Rebughini, M. Bracconi, A. Cuoci, M. Maestri, Catalysis Engineering: From the Catalytic Material to the Catalytic Reactor, in: Joost Frenken, Irene Groot (Eds), '*Operando* Research in Heterogeneous Catalysis', Springer Series in Chemical Physics, **2017**, p. 189.

[5] S. Mitchell, A. J. Martín, J. Pérez-Ramírez, *Nat. Chem. Eng.* **2024**, *1*, 13, https://doi.org/10.1038/s44286-023-00005-1.

[6] M. Tommasi, S. Naz Degerli, G. Ramis, I. Rossetti, *Chem. Eng. Res. Design* **2024**, *201*, 457, https://doi.org/10.1016/j.cherd.2023.11.060.

[7] L. Kiewidt, J. Thöming, *Chem. Eng. Sci*. **2015**, *132*, 59, https://doi.org/10.1016/j.ces.2015.03.068.

[8] H. Ridder, C. Sinn, G. R. Pesch, J. Ilsemann, W. Dreher, J. Thöming, *Rev. Sci. Instrum*. **2021**, *92*, 043711, https://doi.org/10.1063/5.0044795.

[9] M. Nikolic, A. Cesarini, E. Billeter, F. Weyand, P. Trtik, M. Strobl, A. Borgschulte, *Angew. Chem. Int. Ed.* **2023**, *45*, 62, e202307367, https://doi.org/10.1002/anie.202307367.

[10] P. C. H. Mitchell, S. F. Parker, A. J. Ramirez-Cuesta, J. Tomkinson, 'Vibrational Spectroscopy with Neutrons with Applications in Chemistry, Biology, Materials Science and Catalysis'; World Scientific Publishing: Singapore, **2005**. https://doi.org/10.1142/5628

[11] E. H. Lehmann, *NDT&E* **2001**, *16*, 197, https://doi.org/10.1007/978-3-663-11567-0_8.

[12] S.F. Parker, D. Lennon, *Physchem* **2021**, *1*, 95, https://doi.org/10.3390/physchem1010007.

[13] R. G Sachs, E. Teller, *Phys. Rev*. **1941**, *60*, https://doi.org/10.1103/PhysRev.60.18.

[14] S. J. Seestrom, E. R. Adamek, D. Barlow, M. Blatnik, L. J. Broussard, N. B. Callahan, S. M. Clayton, C. Cude-Woods, S. Currie, E. B. Dees, W. Fox, M. Hoffbauer, K. P. Hickerson, A. T. Holley, C. -y. Liu, M. Makela, J. Medina, D. J. Morely, C. L. Morris, R. W. Pattie Jr., J. Ramsey, A. Roberts, D. J. Salvat, A. Saunders, E. I. Sharapov, S. K. L. Sjue, B. A. Slaughter, P. L. Walstrom, Z. Wang, J. Wexler, T. L. Womack, A. R. Young, J. Vanderwerp, B. A. Zeck, *Phys. Rev. C* **2017**, *95*, 015501, https://doi.org/10.1103/PhysRevC.95.015501.

[15] E.R. Carreon Ruiz, J. Lee, M. Strobl, N. Stalder, G. Burca, L. Gubler, P. Boillat, *Sci. Adv.* **2023**, *9*, eadi0586, https://doi.org/10.1126/sciadv.adi0586.

[16] P. Vontobel, E. H. Lehmann, R. Hassanein, G. Frei, *Phys. Rev. B: Condens*. **2006**, *385*, 475, https://doi.org/10.1016/j.physb.2006.05.252.

[17] P. Trtik, et al., *Mater. Res. Proc.* **2020**, *15*, 23

[18] A. Tengattini, N. Kardjilov, L. Helfen, P-A. Douissard, N. Lenoir, H. Markötter, A. Hilger, T. Arlt, M. Paulisch, T. Turek, I. Manke, *Opt Express* **2022**, *25*, 14461, https://doi.org/10.1364/OE.448932.

[19] V. Manzi-Orezzoli, M. Siegwart, M. Cochet, T. J. Schmidt, P. Boillat, *J. Electrochem. Soc.* **2020**, *167* 054503, https://doi.org/10.1149/2.0062005JES.

[20] R. Zboray, P. Trtik, *Flow Measur. & Instr.* **2019**, *66*, 182, https://doi.org/10.1016/j.flowmeasinst.2019.03.005.

[21] A. Kaestner, https://www.youtube.com/watch?v=VESMU7JfVHU

[22] A. G. Dixon, B. Partopour; *Annu. Rev. Chem. Biomol. Eng.* **2020**, *11*, 109, https://doi.org/10.1146/annurev-chembioeng-092319-075328.

[23] B. Fumey, R. Weber, P. Gantenbein, X. Daguenet-Frick, I. Hughes, V. Dorer, *Energy Procedia*, **2015**, *70*, 203, https://doi.org/10.1016/j.egypro.2015.02.116.

[24] B. Fumey, L. Baldini, A. Borgschulte, *Energy Technol*. **2020**, *8*, 2000187, https://doi.org/10.1002/ente.202000187.
[25] B. Fumey, A. Borgschulte, S. Stoller, R. Fricker, R. Knechtle, A. Kaestner, P. Trtik, L. Baldini, *Int. J. Heat Mass Transfer*, **2022**, *182* 121967, https://doi.org/10.1016/j.ijheatmasstransfer.2021.121967.
[26] A. Borgschulte, N. Gallandat, B. Probst, R. Suter, E. Callini, D. Ferri, Y. Arroyo, R. Erni, H. Geerlings, A. Züttel, *Phys. Chem. Chem. Phys.*, **2013**,*15*, 9620, https://doi.org/10.1039/c3cp51408k.
[27] B. T. Carvill, J. R. Hufton, M. Anand, S. Sircar, *AIChE J*., **1996**, *42*, 2765, https://doi.org/10.1002/aic.690421008.
[28] A. Borgschulte, R. Delmelle, R. B. Duarte, A. Heel, P. Boillat, E. Lehmann, *Phys. Chem. Chem. Phys*. **2016**, *18*, 17217, https://doi.org/10.1039/C5CP07686B.
[29] P. Bareschino, G. Piso, F. Pepe, C. Tregambi, E. Mancusi, *Chem. Eng. Sci.* **2023**, *277*, 118876, https://doi.org/10.1016/j.ces.2023.118876.
[30] F. Kiefer, M. Nikolic, A. Borgschulte, P. D. Eggenschwiler, *Chem. Eng. J.*, **2022**, *449*, 137872, https://doi.org/10.1016/j.cej.2022.137872.
[31] D. Linden, T. Reddy, 'Handbook of Batteries', Electronics Book Series, McGraw-Hill **2002**.
[32] J. van Vucht, F. Kuijpers, H. C. Bruning, Philips *Res. Rep*. **1970**, *25*, 133, https://doi.org/10.1016/0022-5088(89)90453-0.
[33] P. Boillat, D. Kramer, B.C. Seyfang, G. Frei, E. Lehmann, G.G. Scherer, A. Wokaun, Y. Ichikawa, Y. Tasaki, K. Shinohara, *Electrochem. Commun*., **2008**, *10*, 546.
[34] E. Ricardo Carreón Ruiz, Jongmin Lee, J. Ignacio Márquez Damián, M. Strobl, G. Burca, R. Woracek, M.- O. Ebert, E. Winter, M. Cochet, L. Höltschi, P. M. Kadletz, M. Zlobinski, A. S. Tremsin, L. Gubler, P. Boillat, *Mater. Today Adv*. **2023**, *19*, 100405, https://doi.org/10.1016/j.mtadv.2023.100405.
[35] J. Disch, L. Bohn, S. Koch, M. Schulz, Y. Han, A. Tengattini, L. Helfen, M. Breitwieser, S. Vierrath, *Nat. Commun.* **2022**, *13*, 6099, https://doi.org/10.1038/s41467-022-33694-y.
[36] J. Terreni, E. Billeter; O. Sambalova, X. Liu, M. Trottmann, A. Sterzi, H. Geerlings, P. Trtik, A. Kaestner, A. Borgschulte, *Phys. Chem. Chem. Phys*. **2020**, *22*, 22979, https://doi.org/10.1039/D0CP03414B.
[37] M. Nikolic, F. Longo, E. Billeter, A. Cesarini, P. Trtik, A. Borgschulte, *Phys. Chem. Chem. Phys*. **2022**, *24*, 27394, https://doi.org/10.1039/D2CP03863C.

License and Terms

The definitive version of this article is the electronic one that can be found at https://doi.org/10.2533/chimia.2024.333